
Star-disk interaction in Classical T Tauri stars

Silvia H. P. Alencar¹

Departamento de Física - ICEx-UFMG, CP. 702, Belo Horizonte, MG, 31270-901, Brazil silvia@fisica.ufmg.br

1 Introduction

Stars are born in molecular clouds. The mechanisms involved in the transformation of a cloud core into a star and the various evolutionary phases that the star-disk systems go through have been the center of attention of many recent studies (see recent reviews from the Protostars and Planets V conference [46]).

The protostar and disk are formed deeply embedded in their original collapsing cloud. From there on, in the case of low-mass stars, most of the stellar mass will be acquired through accretion from the disk. Initially, material still falls from the surrounding envelope to the disk, while the disk accretes material into the star. At the same time, winds, jets and molecular outflows are driven by the young star-disk system and help dissipating the surrounding cloud. When the Pre-Main Sequence (PMS) star becomes optically visible, it is called a T Tauri star (TTS) if its spectral type is later than F or a Herbig Ae/Be star (HAeBe) if it has spectral type between B and F. At that point, the star still accretes from the disk, but at lower accretion rates (typically $\dot{M}_{acc} \sim 10^{-8} M_{\odot} \text{ yr}^{-1}$) than in the protostellar phase.

The gas in the circumstellar disk will eventually vanish, but it is not actually clear what is the main cause of the gas dissipation. It can be just mostly accreted to the star, part of it may go into giant planets, it can also be disrupted by tidal instabilities and gaps created by planet formation or dissipated by UV photoionization by the central star. Some T Tauri stars, known as weak-lined T Tauri stars do not exhibit accretion disks at very early ages (~ 1 Myr) while others, the Classical T Tauri Stars (CTTSs), at the same ages and spectral types still do. Being brief or lasting longer, the star-disk interaction has a significant impact on early stellar evolution. It provides mass through accretion, helps regulate the angular momentum transfer and may be in part responsible for winds and jets observed in young stars.

In this contribution we will focus in accretion processes related to CTTSs. In section 2, we will review the past and present models used to explain the

observed characteristics of CTTSs. We will discuss the recent magnetic field measurements in section 3 and the spectral diagnostics of magnetospheric accretion and accretion powered winds (section 4). We will also emphasize in section 5 the dynamical aspect of magnetospheric accretion and show how the models and simulations are dealing with such a characteristic.

2 Classical T Tauri star models: past and present

Classical T Tauri stars are young, optically visible, low mass stars that show signs of accretion from a circumstellar disk. They are a few million years old at most and still contracting down their Hayashi tracks. CTTSs show Li I in absorption, which is a telltale of youth for low mass stars. They present broad permitted emission lines and they are spectroscopic and photometrically variable. They show ultraviolet (UV), optical and infrared (IR) excesses with respect to the photospheric flux. They have strong magnetic fields (~ 2 kG) and are X-ray emitters. Over the years, as the observational characteristics above were discovered, several models were proposed to explain the CTTS phenomenon.

2.1 Boundary layer models

Lynden-Bell and Pringle (1974) [34] presented the idea that viscous dissipation in disks might be responsible for the IR excess. They also proposed that the UV excess could be produced in a shear equatorial boundary layer between the rapidly rotating disk (at more than 200 km s^{-1} just above the photosphere) and the slowly rotating star ($v \sin i \sim 10 \text{ km s}^{-1}$, typically). In the boundary layer, the accreting material loses its kinetic energy in a series of shocks and emits a luminosity comparable to that released in the rest of the accretion disk, but over a very small area. Therefore the boundary layer must be much hotter than the rest of the disk, and so it will radiate at shorter wavelengths, peaking in the UV. It was only in the 80's that the idea became popular with the observational advances in UV and IR.

However, the boundary layer model (BLM) soon faced several observational challenges that it could not overcome. These models could not explain the inverse P Cygni profiles commonly observed in CTTS emission lines, which show blueshifted emission peaks and redshifted absorption components at $200\text{--}300 \text{ km s}^{-1}$ reaching below the continuum. The redshifted absorption component is thought to come from material that is receding from us towards the star at near free-fall velocities. In the BLM, material is supposed to slow down from the disk to the star, producing small radial velocities.

The BLM also could not explain the spectral energy distribution (the observed flux distribution as a function of wavelength) of many CTTSs that are only fitted by disk models without the inner disk regions (a disk hole). In the BLM, the disk is expected to continue down to the stellar photosphere.

These models had also difficulties to explain why CTTSs are generally found to be slow rotators ($v \sin i \sim 10 \text{ km s}^{-1}$), since the accretion process should only add angular momentum and therefore spin-up the star.

2.2 Wind Models

Wind models were also suggested to explain the CTTSs emission line spectra [22, 23, 42]. These models tended to predict mostly P Cygni profiles (i.e. redshifted emission peaks and blueshifted absorption often going below the continuum) for the main emission lines. Consequently, they had a hard time generating the rather symmetric emission line profiles with blue-shifted features that do not reach the continuum, which are the most commonly observed in the main emission lines of CTTSs. The early wind models also tended to predict upper Balmer lines with strong wind absorption components and could not explain the spectra of many CTTSs that show these lines with very faint or even without blueshifted absorption. Wind models could not produce the observed inverse P Cygni profiles either.

All these arguments against the wind models do not mean that there is no wind in CTTSs, or no wind contribution to the observed profiles of CTTSs. It just indicates that the wind is not the main responsible for the permitted emission line profiles. The narrow blueshifted absorptions, however, remain wind features. They are attributed to cool outflowing gas that is further from the star than the accretion dominated emission.

2.3 Magnetospheric accretion models

Nowadays magnetospheric accretion models are the consensus to explain the many observed characteristics of CTTSs [50, 24, 38, 39]. These models are based on the idea of circumstellar disk accretion onto a magnetized young star. It is assumed that the stellar magnetic field is predominantly dipolar on the large scale and that it is strong enough to disrupt the disk at the so-called truncation radius, typically a few stellar radii from the star, where the magnetic pressure overcomes the ram pressure due to accretion. This forms a magnetospheric cavity (Fig. 1).

The accreting material that goes spiraling down the disk eventually reaches the inner disk region. If it is sufficiently ionized, its motion will then be controlled by the magnetic field. Part of it is ejected in a wind, and part is accreted onto the star along magnetic field lines, forming accretion columns.

As the near free-falling material hits the stellar surface, a strong accretion shock (a hot spot) is produced. The shock emission is responsible for the UV and optical continuum excess, known as veiling. The broad emission lines come from the accelerated material in the accretion columns and forbidden emission lines are formed in the wind. The IR excess comes from the combination of viscous dissipation and reprocessing of stellar and/or accretion radiation by the disk.

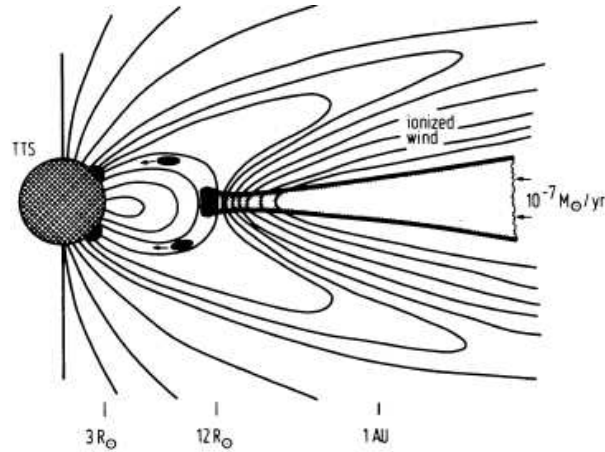


Fig. 1. Sketch of magnetospheric accretion in CTTSs (from Camenzind, 1990 [10])

For accretion to occur, the truncation radius must be smaller than the corotation radius R_{co} (radial distance in the disk where the keplerian angular velocity matches the stellar angular velocity). Only inside R_{co} will the net force allow the material to accrete. Outside R_{co} the stellar angular velocity is greater than the Keplerian velocity, so that any material there which becomes locked to the stellar field lines will experience a centrifugal force that tries to throw the material away from the star (disk-wind).

This is the basic concept of magnetospheric accretion in CTTSs. So to begin with, we need strong stellar magnetic fields.

3 Magnetic Fields measurements: theory vs. observations

Traditional magnetospheric accretion theories suggest that, when the star-disk system is in equilibrium, the stellar rotation rate will be determined by the keplerian rotation rate near the truncation radius. The star is locked to the disk and these are therefore often called disk locking theories. Under the assumption that such an equilibrium situation exists, Königl (1991)[31], Collier Cameron & Campbell (1993)[11] and Shu et al. (1994)[50] have analytically analysed the interaction of a dipolar stellar magnetic field aligned with the stellar rotation axis and the inner accretion disk. Using the equations provided by each of the above cited works, Johns-Krull et al (1999b)[27] obtained analytical expressions for the magnetic field strength in terms of the stellar mass and radius, the rotation period of the star and the mass accretion rate (see eqs. 2, 3 and 4 of [27]). Since these quantities have been estimated for several CTTSs, the models can then predict stellar magnetic field values that can later be compared with values obtained from the observations (cf Fig. 3).

Magnetic field measurements most of the time make use of the Zeeman splitting effect. When an atom is in the presence of a magnetic field, a spectral line is shifted in three components: two σ components, split to either side of the line center and a π component, which is unshifted. The wavelength shift of a σ component is given by:

$$\Delta\lambda = \frac{e}{4\pi m_e c^2} \lambda^2 g B$$

As shown above, the Zeeman shift has a λ^2 dependence, while Doppler line broadening mechanisms have just a λ dependence, so it is a good idea to look for magnetically sensitive lines in the IR in order to enhance the Zeeman effect compared to Doppler broadening. Making use of this characteristic, Valenti & Johns-Krull (2004) [55] fitted synthetic line models with magnetic field to magnetically sensitive Ti I lines in the IR spectra of CTTSs. An example of their analysis is shown in Fig. 2 for the CTTS BP Tau. The model with no magnetic field (single line) does not fit the data, while the model with a distribution of magnetic fields in the stellar surface, going from zero up to 6 kG, with a mean field value of 2.1 kG, gives a very good fit to the observations. In order to constrain non-magnetic broadening mechanisms Valenti & Johns-Krull (2004) [55] also fitted various CO lines that lie near the Ti I lines at 2.3 microns and have negligible Landé factors, which means they are Zeeman insensitive. As can be seen in the bottom panel of Fig. 2, the CO lines are much narrower than the Ti I lines and are well fitted by both the non-magnetic and the magnetic models, as expected. The surface magnetic field distribution of several TTSs has now been measured fitting the IR spectra with synthetic line models [27, 28, 30, 58].

The results presented in Fig. 2 show that the Zeeman broadening of magnetically sensitive lines is sensitive to the distribution of magnetic field strengths, it presents however limited sensitivity to magnetic geometry. On the other hand, circular polarization measurements for individual spectral lines are sensitive to magnetic geometry, but they provide limited information about the total magnetic field strength.

The idea to use circular polarization is that, when viewed along the axis of a magnetic field, the Zeeman σ components are circularly polarized, but with opposite helicity, while the π component is absent. If one magnetic polarity is dominant at the visible surface of the star, net circular polarization is present in Zeeman sensitive lines. In that case, the magnitude of the wavelength shift is proportional to the surface average line of sight component of the magnetic field.

Most magnetospheric accretion models assume that the magnetic fields of TTSs are dipolar. It is true that the higher order multipoles fall off more rapidly than the dipole, so that at the inner edge of the disk, typically at a few stellar radii from the star, the dipole is likely to dominate. But close to the stellar surface, the magnetic field geometry is probably more complicated,

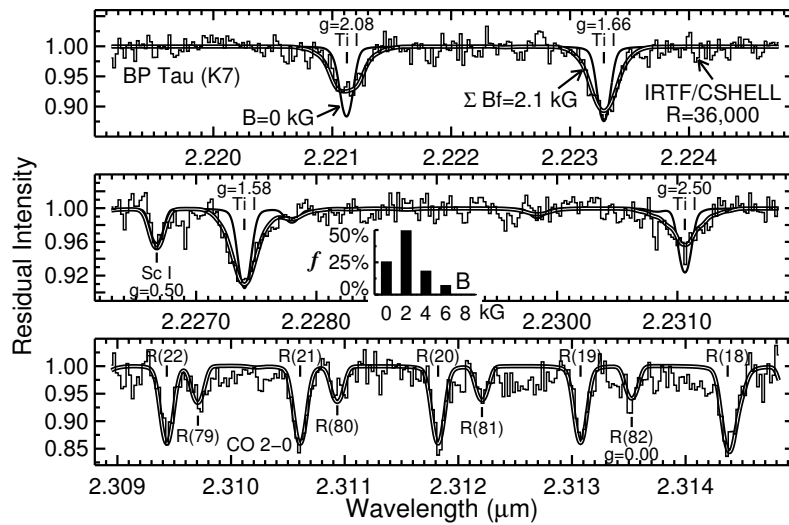


Fig. 2. An IR spectrum of the CTTS BP Tau (histogram) compared with synthetic line models with magnetic fields (doubled curve) and without (single curve). The inset histogram shows the distribution of magnetic fields used over the entire surface in the magnetic models to reproduce the observed spectrum. The Landé-g factor is given for each atomic line. Figure taken from Valenti & Johns-Krull (2004) [55].

with the presence of many multipole components. In support to that idea is the fact that most spectropolarimetric studies of cool stars do not clearly detect circular polarization in photospheric absorption lines (that form all over the surface of the star), within an upper limit of about 100 G [56, 8].

However, Johns-Krull et al. (1999a) [27] detected circular polarization in CTTSs emission lines that form predominantly in the accretion shock. There we are not looking at the whole stellar surface, but we are isolating a small portion of it. The strongest circular polarization signal appears in the narrow emission component of the He I line (5876 Å). In contrast to the photospheric features, which show no net field polarity in the line of sight, the narrow helium emission arises in a region with mean line of sight fields from 1-2.75 kG that exhibit a high degree of organization, indicating that a single polarity dominates in the He I formation region. Valenti & Johns-Krull (2004) [55] have further measured the line of sight component of the magnetic field on six consecutive nights for four stars. The measured values vary smoothly on rotational timescales, implying a lack of symmetry about the rotation axis in the accretion or the magnetic field, or both. Simple models consisting of a single spot at a given latitude that rotates with the star fit the data quite well.

The complicated surface topology of magnetic fields in CTTSs results in no net polarization in photospheric absorption lines. However, the accreting

material apparently follows the dominant polarity of the field at the inner disk edge, so that emission lines formed in the accretion shock preferentially illuminate a dominant polarity component of the field, producing substantial circular polarization in these emission lines. The dominant polarity component near the truncation radius is expected to be the dipole component, as predicted by the magnetospheric theories, if the truncation radius is far enough for it to dominate over the others. However, Subu Mohanty and Scott Gregory have shown in their talks at the school that for small truncation radii, accretion is likely to occur along non-dipolar field lines.

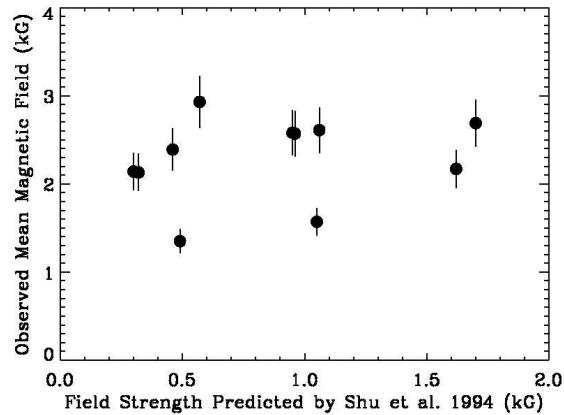


Fig. 3. Observed mean magnetic field strength as a function of the predicted field strength for the theory of Shu et al. (1994) [50]. There is no statistically significant correlation between the observed and predicted magnetic field strengths. Figure taken from Bouvier et al. (2006) [7].

In Fig. 3 are shown the most recent compilation of mean magnetic field intensities measured by Johns-Krull and collaborators together with the predicted field strengths from Shu et al. (1994) [50]. We can readily see that the mean fields do not agree with the theory. A hint to why we do not see such a correlation may come from the field topology measurements, since they indicate the magnetic field on the TTSS surface is not globally dipolar. The dipole component may then actually be much less important than predicted by the theories. There is therefore the need to include non-dipole fields in the magnetospheric accretion theory to try to reconcile theory and observations. This was done by Johns-Krull & Gafford (2002) [29] who compared the relationships predicted by magnetospheric accretion theories among stellar mass, radius, rotation period and disk accretion rate and the observed relations from several studies of CTTSS. They were only able to reproduce the observed cor-

relations after including non-dipole field topologies in the model of Ostriker & Shu (1995).

4 Spectral diagnostics of magnetospheric accretion

4.1 Emission-line profiles

The magnetic field distribution and topology is one of the most important ingredients to understand and correctly describe the magnetospheric accretion process in CTTSs. There are, however, several other diagnostics of magnetospheric accretion, such as the permitted emission line profiles of CTTSs that are supposed to be formed in the accretion funnel.

These emission line profiles show a wide variety of morphologies (symmetric, double-peaked, P Cygni, inverse P Cygni) and they can vary from one type to another in a single star. In common to all types of profiles is the broad line width with several 100 km s^{-1} indicative of bulk motion of the circumstellar material. The emission line profiles are important because they encode both geometrical and physical information on the accretion process and its rate. So a straightforward idea is to use them to test and refine the magnetospheric accretion models.

The standard magnetospheric accretion models assume an axisymmetric geometry in which the density structure along the funnel is calculated using a steady mass accretion rate and free-fall along dipolar field lines, which come from a geometrically thin but optically thick disk at a range of radii inside the co-rotation radius. It is generally assumed that the kinetic energy of the accreting material is completely thermalized.

The radiative transfer calculations are typically performed with the Sobolev approximation ie assuming that the contributions to a spectral line formation at any given frequency occur locally, that is valid under the assumption of high velocity gradients. The temperature structure, which is a significant parameter, is unfortunately poorly constrained. A simple adjustable volumetric heating rate combined with a schematic radiative cooling rate, which leads to a temperature structure that goes as the reciprocal of the density is often adopted [24, 38, 39, 53]. The magnetospheric accretion models may also include rotation and line damping.

Actually the models are able to compute a huge variety of profiles, as observed, and the calculations are performed for several different atomic species, such as hydrogen, sodium, calcium and oxygen. Several hydrogen transitions in the optical and IR have also been calculated.

Even with all the simplifications and assumptions that are made in the models, it is fair to say that the magnetospheric accretion models do a very good job in reproducing the main observed characteristics of the permitted emission line profiles (see Fig. 4), such as the broad line widths and the occasional inverse P Cygni profiles [38, 39] The models are also often able to

reproduce several lines simultaneously, which allows to better constrain the many fitting parameters. Care must be taken to determine the accretion and magnetospheric parameters with only one line like $H\alpha$, which is the most commonly used, since it is vulnerable to have contributions from outflows (see [3, 2]) and it may also be significantly spatially extended.

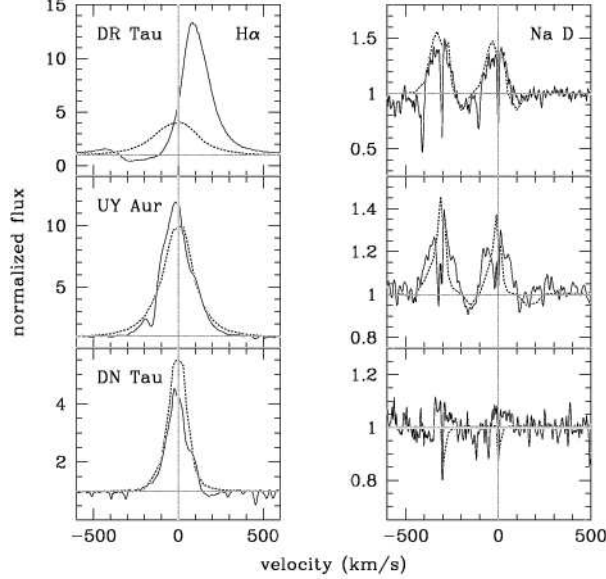


Fig. 4. Observed (solid lines) and magnetospheric accretion model (dotted lines) permitted emission line profiles of three CTTSs. We see that the magnetospheric accretion models reproduce very well the emission part of the profiles but do not reproduce the blueshifted absorptions in $H\alpha$ and NaD of any of the stars nor the shape and intensity of the $H\alpha$ line of a high mass accretion rate CTTSs like DR Tau. Those features are believed to be due to winds. Figure taken from Muzerolle et al. (2001)[39].

Lately the magnetospheric accretion model has been used to determine mass accretion rates across the mass spectrum, from Herbig Ae stars, UX Ori being a good example [40] and also to very low mass objects and brown dwarfs [41].

In general, the fit to the emission component of the observed line profiles is quite good but there are exceptions like DR Tau, which is a high mass accretion rate system (see Fig. 4). In that case, it has been suggested by Muzerolle et al. (2001) [39] that the wind can give an important contribution to the emission line profile.

4.2 Accretion driven winds

It is widely accepted that winds are important ingredients of star formation, but the wind contribution to the line profiles of CTTSs has not been very much studied in the last years, because of the apparent importance of accretion to the observed profiles.

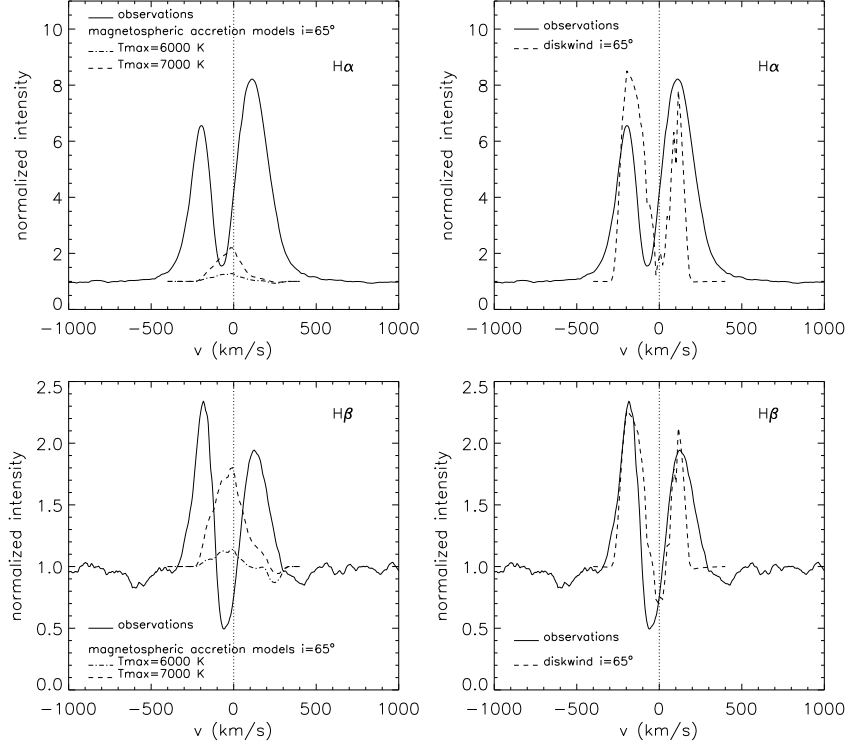


Fig. 5. RW Aur mean observed line profiles are shown as solid lines. *Left:* magnetospheric accretion profiles (dashed and dash-dotted lines). *Right:* disk-wind profiles (dashed lines). From Alencar et al. (2005).

Alencar et al. (2005) [2] have recently shown that the observed emission profiles of RW Aur, a high mass accretion rate CTTS, can have a strong wind contribution, as predicted by Muzerolle et al. (2001) [39] for such star-disk systems. In Fig. 5 we show the magnetospheric accretion and disk wind profiles compared with mean H α and H β observations of RW Aur. We can see that the disk wind models fit better the observations, indicating that, in this case, the wind contribution is important. Alencar et al. (2005) [2] calculated the magnetosphere and wind models separately, while to be consistent, the accretion and wind contributions must be calculated at the same time, as

Kurosawa et al. (2005, 2006) [32, 33] have recently done for the first time. They computed hybrid models where both effects are taken into consideration and they are able to reproduce all types of emission line profiles observed in CTTs (see Fig. 5 of [7]). Only hybrid models are able to simultaneously reproduce the emission and the narrow blueshifted absorption, which is attributed to cool outflowing gas that is further from the star than the accretion dominated emission. The narrow blueshifted absorption features exhibit a great variety in depth, width and velocity from one star to another, although there is a general tendency for them to be more prominent in stars with high mass accretion rates [14], indicating that these are not purely stellar winds but are powered by an accretion/outflow connection.

Recently another spectral wind diagnostic has been identified with the confirmation of the presence of a hot helium wind among stars with high accretion and outflow rates provided by profiles in the near infrared triplet line of He I 10830 Å [15].

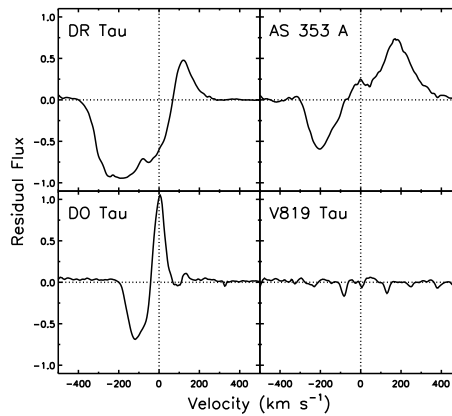


Fig. 6. Observed He I 10830 Å line profiles of 3 CTTs (DR Tau, AS 353 A, DO Tau) and 1 WTTS (Suzan Edwards, private communication).

In Fig. 6, kindly provided by Suzan Edwards prior to publication, we see the He I 10830 Å line of three CTTs (DR Tau, AS 353 A, DO Tau) and one WTTS (V819 Tau). The CTTs present very impressive P Cygni profiles with blueshifted absorptions going way below the continuum in a spectral region where the continuum is mostly due to the star. At 1 micron the accretion shock does not contribute to the continuum and the IR excess from the disk is still rising and does not contribute much either. In Figure 6 we can see that for DR Tau, AS 353A and DO Tau the blueshifted absorption reaches then into the stellar continuum over a continuous and broad velocity range going from near the stellar rest velocity to the terminal wind velocity. In order to

have helium emission we further need high temperatures ($T > 10\,000$ K). So the acceleration region of the helium wind is close to the star, occulting a significant portion of it, in a region of high temperature.

One possibility is that the helium wind comes from polar/coronal regions. This would allow magnetospheric accretion funnels to co-exist with such a hot wind. It would actually be difficult for disk wind material to absorb the radiation from the stellar disk at all velocities, from the rest to the terminal wind speed. As extreme examples, TW Hya and T Tau are pole on CTTSs and they also present the He I (10830 Å) line with the same strong and extended blueshifted absorptions (see [12]). In those cases it is almost impossible for an inner wind to be of disk origin and produce such absorptions of the stellar continuum.

If the wind arises from the stellar coronae it would not be a normal stellar wind but rather an accretion powered stellar wind, since this wind is strongest in stars with the highest mass accretion rates. Low mass accretion rate CTTSs, like AA Tau, show He I (10830 Å) profiles that are compatible with a disk wind with narrow blueshifted absorptions much like in H α (Suzan Edwards, private communication) and WTTSs do not show any absorption or emission at all, as can be seen in Fig. 6 for V819 Tau.

The picture of the star-disk interaction in the PMS that is emerging from observational results includes magnetospheric accretion, a disk wind, and an accretion powered stellar wind, as discussed by Matt & Pudritz (2005) [37] and by Ferreira et al. (2006) [18] and shown schematically in Figure 1.

4.3 Accretion shock evidences

Another key parameter of the magnetospheric accretion model is the presence of accretion shocks that create hot spots at the stellar surface where the infalling material reaches the star. Hot spots were initially inferred from rotational modulation of light curves by Bouvier et al. (1995) [4]. In order to ensure that the photometric modulation was mainly caused by hot spots and not by cold ones, the temperature and minimum size of the spots responsible for the the stellar brightness modulation were derived by comparing the observed amplitude of variability in different wavelengths with hot and cool spot models calculated with various temperatures and spot sizes. Hot spot models failed to reproduce the observations of WTTSs, while both hot and cool spots can be responsible for the observed modulation of CTTSs. Half of the observed CTTSs in Bouvier et al. (1995) [4] had amplitudes consistent with a modulation by cool spots, and half by hot spots. Their conclusion was that CTTSs present both cool and hot spots, while WTTSs only show evidence for cool spots.

Another evidence for accretion shocks comes from the successful fitting of the UV and optical excesses observed in CTTSs by accretion shock models ([9], [21]). The shape of the excess can be understood as optically thick emission from the heated photosphere below the shock and optically thin emission

from the preshock and postshock regions. According to the models, the accretion shock will initially have $T \sim 10^6$ K and emit in soft X-rays, which are reprocessed both by the accretion stream and the stellar photosphere, accounting for the optical and UV continuum emission. An important product of such a fitting is the reliable determination of mass accretion rates, which can later be used to calibrate other accretion diagnostics that are easier to measure than the UV excess, such as the luminosity of emission lines like Paschen β .

4.4 X-ray emission

Young stars are bright in X-rays from Class I to Class III stages. They can be up to 10^4 times more luminous than the Sun in X-rays, which are thought to be mainly produced by magnetic reconnection flares [16].

In the magnetic reconnection, oppositely directed magnetic field lines are brought together into a strong eddy that pushes away the gas. The magnetic reconnection changes the topology of magnetic fields by breaking magnetic field lines and reconnecting them in a different way. In doing so, it can liberate magnetic energy into other forms such as kinetic energy, heat and light.

Recently a collaboration known as the Chandra Orion Ultradeep Project (COUP) lead by Eric Feigelson (Penn State Univ.) has obtained 13 days of observations of the Orion Nebular Cluster with the Chandra X-ray observatory (ApJS Volume on the COUP project [17, 44]). They confirmed that there is no X-ray quiet young population and that the X-rays from young stars are mainly of enhanced solar-like coronae origin, but they can also have contributions of soft X-rays from accretion columns and of intense flares from the reconnection of field lines taking part in the magnetic star-disk interaction. Such intense flares are predicted by numerical simulations of the star-disk interaction, where differential rotation between the stellar field lines and the inner disk are shown to lead to the lines expansion, opening and reconnection (see Sect. 5.1).

CTTSs are known to be less X-ray active than WTTSs but this difference is not due to the fact that CTTSs rotate more slowly than WTTSs, since in the PMS no activity-rotation is observed, while it is in the later phases of stellar evolution [44]. The reason for such a difference is still under debate and could be due to X-ray absorption by circumstellar features around CTTSs. Accretion could also change the magnetosphere itself, loading the field lines and therefore not allowing the high density plasma to reach very high temperatures needed to emit X-rays. Another possibility under discussion is that accretion may change the stellar structure, inhibiting the dynamo process and therefore affecting the rising of magnetic field lines at the stellar surface [44].

5 The future of CTTS models

In terms of observational evidences, we can say that magnetospheric accretion is overall in a robust ground. We have seen that strong magnetic fields are present in CTTSs [55]. It was shown that accretion columns are inferred through the observation of inverse P Cygni profiles with redshifted absorptions at several hundred km s^{-1} [13], which indicates that the gas is accreted onto the star from a distance of a few stellar radii and we saw that emission lines are formed, at least partially, in accretion funnel flows [24, 38, 39]. Accretion shocks are inferred from the rotational modulation of light curves by bright surface spots [4] and accretion shock emission models have also successfully reproduced the observed spectral energy distribution of optical and UV excess [9, 21].

However some caveats do apply to the models and there are aspects such as the variability of the accretion process that are not taken into account by the very good but steady state, axisymmetric accretion models.

The first and probably one of the most important problems is that the temperature structure of the accretion flow is essentially arbitrary, and this has a significant impact on the line source functions and consequently on the profiles themselves.

Martin (1996) [35] showed that in the funnel, the heating is dominated by adiabatic compression and the cooling comes mainly from free-free emission (bremsstrahlung radiation) and line emission from ions such as CaII and MgII. The temperature structure he obtained is quite different from the one commonly used in the magnetospheric accretion models. However, the somewhat arbitrary temperature law proposed by Hartmann et al. (1994) [24] yields profiles that definitely look like the observations, while the Martin (1996) one, which was calculated consistently, does not. There is therefore the need to further analyse the heating and cooling processes that take place in the accretion funnel.

Another important point that the standard models do not deal with, is that the accretion process is very variable. Steady state axisymmetric models cannot obviously explain the observed variability.

SU Aur is a typical example of CTTS that shows variable emission lines [25, 43]. It also shows periodic infall and outflow signatures that are 180 degrees out of phase, indicating that the wind is strongest when the infall is weakest. This can be explained by a magnetospheric accretion model with an inclined dipole field with respect to the rotation axis (non-axisymmetric) in which accretion and outflow are naturally favored in opposite phases.

TW Hya is a pole-on CTTS that, despite of that, presents a daily variability of its emission line profiles [1]. In that case, even an inclined dipole cannot easily explain such variabilities and there is evidence therefore for non-steady accretion towards the star, a feature that the standard magnetospheric accretion models do not take into account.

Overall, the accretion/ejection processes appear to be dynamical on several timescales. It is variable in hours for non-steady accretion, like seen in the veiling variability of RU Lup during a single night [52]. In weeks, for rotational modulation, like SU Aur discussed before, and like the veiling variability of AA Tau [5]. These week-long variabilities are most likely due to an inclined dipole, causing accretion to be periodically favored at certain phases. Accretion is variable in months, for global instabilities of the magnetosphere. Due to differential rotation between the star and the disk, numerical models have shown that the magnetosphere is expected to expand, open and eventually reconnect [19, 20, 36]. It was also shown that this expansion can be measured observationally by the projected radial velocity of the redshifted absorption component of $H\alpha$, which is formed in the funnel flow [5]. This was observed for AA Tau, as the radial velocity of the redshifted component decreases in a few rotational periods. At the lowest radial velocity level, accretion is inhibited (inflated magnetosphere). The observed veiling then goes to zero and the flux in the lines too. A few days later (maybe reconnection) everything is back again. The accretion/ejection process is also observed to be variable in years from outbursts like EXORs and FU Ori, a recent example being the McNeil nebula [45].

5.1 Dynamical models

The simplest extension to the standard magnetospheric accretion models, in order to investigate the rotational profile variability, is to brake the axisymmetry of the dipole, leaving, for example, curtains of accretion in azimuth, but still keeping the magnetic and rotation axis aligned. Such models were proposed to explain the variability of the observations [51] and are predicted by 3D MHD simulations [48]. Symington et al. (2005) [53] calculated such models and saw that the line profiles overall agree with the observations but they ended up with a variability much larger than usually observed in CTTSs. They suggest that the magnetosphere has probably a high degree of axisymmetry broken by higher density streams that produce the observed variability.

A more complicated but very interesting view of the star-disk interaction has recently emerged from MHD simulations. Romanova et al. (2002) [47] performed impressive MHD simulations of stellar magnetic field and disk interactions in quiescent regime. They calculated 2D MHD simulations of disk accretion to a rotating aligned dipole and showed that funnel flows, where matter flows out of the disk plane and essentially free-falls along the stellar magnetic field lines, are a robust feature of disk accretion to a dipole. In the simulations, which run up to more than 60 Keplerian periods near the inner disk truncation radius, the disk, represented by a “density structure”, truncates and a funnel flow forms near the truncation radius, where the magnetic pressure of the dipole is comparable to the kinetic plus thermal pressure of the accreting material. Some outflow by centrifugal force is present in the simulations and seen to be quasi periodic.

Romanova et al. (2003) [48] also did 3D ideal MHD simulations of the disk accretion to a slowly rotating star with an inclined dipole magnetic field. In these simulations, matter is shown to accrete to the inclined dipole forming non-axisymmetric structures in the stellar magnetosphere. The simulations show that the flow of matter has different shapes at different density levels. The low density part of the flow covers almost the entire magnetosphere, while the larger density regions of the flow accrete in streams. The streams may obscure the light emitted from the stellar surface or from hotspots at the surface of the star, thereby causing stellar variability. The inner regions of the disk often become warped or tilted as the system evolves, as predicted by Terquem & Papaloizou (2000) [54].

Another result of the numerical simulations is the presence of a dynamical interaction between the disk and the stellar magnetosphere. Several simulations have shown that differential rotation along the field lines between the star and the inner disk region leads to the lines expansion, opening and reconnection [19, 20, 36, 49, 57]. When the magnetic field reconnects, strong X-ray flares can be produced. After the reconnection the initial magnetospheric configuration is restored. The timescale for this to occur is of a few rotation periods, determined by the diffusion of the magnetic flux through the inner regions of the disk. That is apparently what was detected in the AA Tau observing campaigns by Bouvier et al. (2003, 2005) [5, 6], but those are the only datasets that allowed to investigate these results. There is therefore the need for longer observing campaigns of CTTSs combining photometry, spectroscopy and polarimetry to investigate the time variability of the magnetospheric accretion and the star-disk interaction in a timescale of weeks to months.

6 Conclusions

The general picture that is emerging nowadays of a CTTS is that of an interacting star-disk system composed of a young magnetized star and its circumstellar disk. The young star has a strong magnetic field that presents a complex topology at the surface and interacts with the circumstellar disk through dipole or multipole field lines, depending whether the disk truncation radius is close to the star (multipoles) or far enough from the star for the dipole to dominate. Magnetospheric accretion, with the overall characteristics predicted by magnetospheric accretion models, is a robust feature in CTTSs, supported nowadays by several observational evidences such as the presence of strong magnetic fields (~ 2 kG), the presence of accretion shocks, the observation of redshifted absorptions from infalling material near free-fall velocities and strong emission lines formed in accretion columns. Accretion also seems to be the driving source of hot stellar winds and disk winds, since such wind signatures are prominent in stars with high mass accretion rates. Disk Winds, accretion-powered stellar winds and magnetospheric accretion apparently co-

exist in CTTSs. Accretion and ejection are then strongly related processes and models that try to explain CTTSs should take both into account.

The star-disk interaction is very dynamical on several timescales (from hours to weeks, months and years) and is mediated by the stellar magnetic field, as evidenced by synoptic studies of CTTSs and by the recent MHD simulations of the star-disk interaction. There is nowadays the need for month-long observational campaigns of CTTSs in order to better understand the dynamics of the star-disk interaction and to test the predictions of the MHD simulations.

Acknowledgements I thank the organisers for a very enjoyable school and JETSET and CNPq (grant 201228/04-1) for financial support. I would also like to thank Suzan Edwards for Figure 6 and many explanations on accretion driven stellar winds, and the PPV team (Jérôme Bouvier, Chris Johns-Krull, Tim Harries and Marina Romanova) for the discussions that, in most part, lead to this contribution.

References

1. S.H.P. Alencar, C. Batalha: ApJ, **571**, 378
2. S.H.P. Alencar, G. Basri, L. Hartmann, & N. Calvet: A&A, **440**, 595
3. I. Appenzeller, C. Bertout, & O. Stahl: A&A, **434**, 1005 (2005)
4. J. Bouvier, E. Covino, O. Kovo, et al.: A&A, **299**, 89 (1995)
5. J. Bouvier, et al.: A&A, **409**, 169 (2003)
6. J. Bouvier, T. Bouvier, S.H.P. Alencar, C. Dougados, C.: Magnetospheric Accretion-Ejection Processes in the CTTS AA Tau. In: *Protostars and Planets V*. LPI Contribution No. 1286., p.8150, 8150
7. J. Bouvier, S.H.P. Alencar, T.J. Harries, C.M. Johns-Krull, M.M. Romanova: Magnetospheric accretion in classical T Tauri stars. In: *Protostars and Planets V*, ed by B. Reipurth, D. Jewitt, K. Keil (University of Arizona Press, Tucson, 2006) in press
8. E.F. Borra, G. Edwards, M. Mayor: ApJ, **284**, 211 (1984)
9. N. Calvet, E. Gullbring: ApJ, **509**, 802 (1998)
10. M. Camenzind: Reviews of Modern Astronomy, **3**, 234 (1990)
11. A. Collier Cameron, & C. G. Campbell: A&A, **274**, 309 (1993)
12. A.K. Dupree, N.S. Brickhouse, G.H. Smith, J. Strader: ApJ, **625**, L131 (2005)
13. S. Edwards, P. Hartigan, L. Ghandour, C. Andriulis: AJ, **108**, 1056 (1994)
14. S. Edwards: Ap&SS, **287**, 47 (2003)
15. S. Edwards, W. Fischer, J. Kwan, L. Hillenbrand, L., A.K. Dupree: ApJ, **599**, L41 (2003)
16. E.D. Feigelson, T. Montmerle: ARA&A, **37**, 363 (1999)
17. E.D. Feigelson, et al.: ApJS, **160**, 379 (2005)
18. J. Ferreira, C. Dougados, S. Cabrit: A&A, in press (2006) **261**, 279 (1982)
19. A.P. Goodson, R.M. Winglee, K.-H. Boehm: ApJ, **489**, 199 (1997)
20. A.P. Goodson, R.M. Winglee: ApJ, **524**, 159 (1999)
21. E. Gullbring, N. Calvet, J. Muzerolle, L. Hartmann: ApJ, **544**, 927 (2000)
22. L. Hartmann, S. Edwards, E. Avrett: ApJ, **261**, 279 (1982)

23. L. Hartmann, N. Calvet, E. Avrett, R. Loesler: ApJ, **349**, 168 (1990)
24. L. Hartmann, R. Hewett, N. Calvet: ApJ, **426**, 669 (1994)
25. C.M. Johns, G. Basri: ApJ, **449**, 341 (1995)
26. C.M. Johns-Krull, J.A. Valenti, C. Koresko: ApJ, **510**, L41 (1999a)
27. C.M. Johns-Krull, J.A. Valenti, C. Koresko: ApJ, **516**, 900 (1999b)
28. C.M. Johns-Krull, J.A. Valenti, S. H. Saar, A. P. Hatzes: ASP Conf. Ser.: Magnetic Fields Across the Hertzsprung-Russell Diagram, ed by G. Mathys, S. K. Solanki, and D. T. Wickramasinghe. (Astronomical Society of the Pacific, San Francisco) 248, 527
29. C.M. Johns-Krull, A.D. Gafford: ApJ, **573**, 685 (2002)
30. C.M. Johns-Krull, J.A. Valenti, S.H. Saar: ApJ, **617**, 1204 (2004)
31. A. Koenigl: ApJ, **370**, L39 (1991)
32. R. Kurosawa, T.J. Harries, N.H. Symington: Formation of H-alpha from Classical T Tauri Stars: The Disc, Wind, and Accretion Hybrid Model. In: *Protostars and Planets V*. LPI Contribution No. 1286., p.8412, 8412
33. R. Kurosawa, T.J. Harries, N.H. Symington: MNRAS, in press (2006)
34. D. Lynden-Bell, & J. E. Pringle: MNRAS**168**, 603 (1974)
35. S.C. Martin: ApJ, **470**, 537
36. S. Matt, A.P. Goodson, R.M. Winglee, K.-H. Bohm: ApJ, **574**, 232
37. S. Matt, R.E. Pudritz: ApJ, **632**, L135 (2005)
38. J. Muzerolle, L. Hartmann, N. Calvet: AJ, **116**, 455 (1998)
39. J. Muzerolle, N. Calvet, & L. Hartmann: ApJ**550**, 944 (2001)
40. J. Muzerolle, P. D'Alessio, N. Calvet, & L. Hartmann: ApJ, **617**, 406 (2004)
41. J. Muzerolle, K. L. Luhman, C. Briceño, L. Hartmann, N. Calvet: ApJ, **625**, 906 (2005)
42. A. Natta, & C. Giovanardi: ApJ, **356**, 646 (1990)
43. P.P. Petrov, E. Gullbring, I. Ilyin, et al.: A&A, **314**, 821 (1996)
44. T. Preibisch, et al.: ApJS, **160**, 401 (2005)
45. B. Reipurth, C. Aspin: ApJ, **606**, L119 (2004)
46. B. Reipurth, D. Jewitt, K. Keil *Protostars and Planets V*, ed by B. Reipurth, D. Jewitt, K. Keil (University of Arizona Press, Tucson, 2006) in press
47. M.M. Romanova, G.V. Ustyugova, A.V. Koldoba, R.V.E. Lovelace: ApJ, **578**, 420 (2002)
48. M.M. Romanova, G.V. Ustyugova, A.V. Koldoba, J.V. Wick, R.V.E. Lovelace: ApJ, **595**, 1009 (2003)
49. M.M. Romanova, G.V. Ustyugova, A.V. Koldoba, R.V.E. Lovelace: ApJ, **616**, L151 (2004)
50. F. Shu, J. Najita, E. Ostriker, et al: ApJ, **429**, 781 (1994)
51. K. Smith, G.F. Lewis, I.A. Bonnell, J.P. Emerson: A&A, **378**, 1003 (2001)
52. H.C. Stempels, N. Piskunov: A&A, **408**, 693 (2003)
53. N.H. Symington, T.J. Harries, R. Kurosawa: MNRAS, **356**, 1489 (2005)
54. C. Terquem, & J. C. B. Papaloizou: A&A, **360**, 1031 (2000)
55. J. A. Valenti, & C. M. Johns-Krull: Ap&SS, **292**, 619 (2004)
56. S. S. Vogt: ApJ, **240**, 567 (1980)
57. B. von Rekowski, B., A. Brandenburg: A&A, **420**, 17 (2004)
58. H. Yang, C.M. Johns-Krull, J.A. Valenti, : ApJ, **635**, 466 (2005)